J|A|C|S
ARTICLES
Published on Web 06/29/2005

Selective Zinc Sensor Molecules with Various Affinities for Zn^{2+}, Revealing Dynamics and Regional Distribution of Synaptically Released Zn^{2+} in Hippocampal Slices

Kensuke Komatsu,[†] Kazuya Kikuchi,*[,†,‡] Hirotatsu Kojima,[†] Yasuteru Urano,[†,‡] and Tetsuo Nagano*[,†]

Contribution from the Graduate School of Pharmaceutical Sciences, The University of Tokyo, 7-3-1 Hongo, Bunkyo-ku, Tokyo 113-0033, Japan, and Presto, JST Agency, Honcho, Kawaguchi-shi, Saitama 332-0012, Japan

Received January 17, 2005; E-mail: tlong@mol.f.u-tokyo.ac.jp; kkikuchi@mol.f.u-tokyo.ac.jp

Abstract: We have developed a series of fluorescent Zn^{2+} sensor molecules with distinct affinities for Zn^{2+}, because biological Zn^{2+} concentrations vary over a wide range from sub-nanomolar to millimolar. The new sensors have K_d values in the range of $10^{-8}-10^{-4}$ M, compared with 2.7 nM for ZnAF-2. They do not fluoresce in the presence of other biologically important metal ions such as calcium or magnesium, and they can detect Zn^{2+} within 100 ms. In cultured cells, the fluorescence intensity of ZnAF-2 was saturated at low Zn^{2+} concentration, while that of ZnAF-3 ($K_d = 0.79\ \mu M$) was not saturated even at relatively high Zn^{2+} concentrations. In hippocampal slices, we measured synaptic release of Zn^{2+} in response to high-potassium-induced depolarization. ZnAF-2 showed similar levels of fluorescence increase in dentate gyrus (DG), CA3 and CA1, which were indistinguishable. However, ZnAF-3 showed a fluorescence increase only in DG. Thus, by using a combination of sensor molecules, it was demonstrated for the first time that a higher Zn^{2+} concentration is released in DG than in CA3 or CA1 and that we can easily visualize Zn^{2+} concentration over a wide range. We believe that the use of various combinations of ZnAF family members will offer unprecedented versatility for fluorescence-microscopic imaging of Zn^{2+} in biological applications.

Introduction

For over a century, zinc (Zn^{2+}) has been known as an essential trace element, acting as a structural component of proteins or in the catalytic site of enzymes.[1] In general, Zn^{2+} is tightly associated with proteins and peptides. However, recent advances in cell biology have revealed a fraction of Zn^{2+} that is free or chelatable in some organs (brain,[2] pancreas,[3] and spermatozoa[4]). In the brain, a considerable amount of chelatable Zn^{2+} is sequestered in the vesicles of presynaptic neurons and is released when the neurons are active.[5] Zn^{2+} is also associated with neuronal disorders,[6] though its role in them is poorly understood. So there is much interest in its detection in vivo, where its concentration varies from 10^{-10} M in the cytoplasm[7] to 10^{-4} M in some vesicles.[8] However, the lack of appropriate detecting tools, especially for such a broad concentration range, hinders further investigation of this spectroscopically silent metal ion.

Fluorescent sensor molecules offer useful information about chelatable Zn^{2+} in cellular systems, because we can study the concentration or distribution of Zn^{2+} in real time,[9] and fluorescence imaging of Zn^{2+} has become a widely and frequently used technique. The first reported sensor molecules for cellular Zn^{2+} were arenesulfonamides of 8-aminoquinoline, such as TSQ [10] and Zinquin.[11] They form 1:2 complexes with Zn^{2+}, emitting strong fluorescence on UV excitation. Since then, various kinds of fluorescent Zn^{2+} sensor molecules have been developed and examined, such as TSQ derivatives,[12] peptide or protein-based sensors,[13] sensors for ratiometric measurement,[14] and others.[15] Above all, various fluorescein derivatives were introduced: NGs,[16] ZPs,[17] FluoZins,[18] ZnAFs,[19] and others.[20] Fluorescein derivatives have many advantages over

[†] The University of Tokyo.
[‡] JST Agency.

(1) (a) Vallee, B. L.; Falchuk, K. H. *Physiol. Rev.* **1993**, *73*, 79−118. (b) Berg, J. M.; Shi, Y. G. *Science* **1996**, *271*, 1081−1085.
(2) (a) Frederickson, C. J. *Int. Rev. Neurobiol.* **1989**, *31*, 145−238. (b) Frederickson, C. J.; Bush, A. I. *Biometals* **2001**, *14*, 353−366. (c) Li, Y.; Hough, C.; Sarvey, J. *Sci. STKE* **2003**, *182*, 19.
(3) (a) Zalewski, P. D.; Millard, S. H.; Forbes, I. J.; Kapaniris, O.; Slavotinek, A.; Betts, W. H.; Ward, A. D.; Lincoln, S. F.; Mahadevan, I. *J. Histochem. Cytochem.* **1994**, *42*, 877−884. (b) Qian, W. J.; Gee, K. R.; Kennedy, R. T. *Anal. Chem.* **2003**, *75*, 3468−3475.
(4) Zalewski, P. D.; Jian, X.; Soon, L. L. L.; Breed, W. G.; Seamark, R. F.; Lincoln, S. F.; Ward, A. D.; Sun, F. Z. *Reprod., Fertil. Dev.* **1996**, *8*, 1097−1105.
(5) (a) Assaf, S. Y.; Chung, S. H. *Nature* **1984**, *308*, 734−736. (b) Howell, G. A.; Welch, M. G.; Frederickson, C. J. *Nature* **1984**, *308*, 736−738.
(6) Bush, A. I. *Curr. Opin. Chem. Biol.* **2000**, *4*, 184−191.
(7) (a) Canzoniero, L. M. T.; Sensi, S. L.; Choi, D. W. *Neurobiol. Dis.* **1997**, *4*, 275−279. (b) Outten, C. E.; O'Halloran, T. V. *Science* **2001**, *292*, 2488−2492. (c) Thompson, R. B.; Peterson, D.; Mahoney, W.; Cramer, M.; Maliwal, B. P.; Suh, S. W.; Frederickson, C.; Fierke, C.; Herman, P. *J. Neurosci. Methods* **2002**, *118*, 63−75. (d) Finney, L. A.; O'Halloran, T. V. *Science* **2003**, *300*, 931−936.
(8) Frederickson, C. J.; Klitenick, M. A.; Manton, W. I.; Kirkpatrick, J. B. *Brain Res.* **1983**, *273*, 335−339.
(9) Mason, W. T. *Fluorescent and Luminescent Probes for Biological Activity*; 2nd ed.; Academic Press: New York, 1999.
(10) Frederickson, C. J.; Kasarskis, E. J.; Ringo, D.; Frederickson, R. E. *J. Neurosci. Methods* **1987**, *20*, 91−103.
(11) Zalewski, P. D.; Forbes, I. J.; Betts, W. H. *Biochem. J.* **1993**, *296*, 403−408.

Zinquin. The high quantum yield in aqueous solution provides high sensitivity in the cellular environment, and the excitation wavelength in the visible range minimizes cell damage during irradiation. These sensors have led to great advances in Zn^{2+} biology, and further development of sensor molecules would be very valuable.[21]

We set out several criteria for developing novel fluorescent Zn^{2+} sensor molecules. First, for intensity-based measurement, the sensor should have no signal in the absence of Zn^{2+}, and the signal should increase in the presence of Zn^{2+} in an all-or-none fashion. Second, the sensor should be selective for Zn^{2+}, without interference by biologically important metal ions, such as Ca^{2+} or Mg^{2+}. Third, complexation and decomplexation with Zn^{2+} should be rapid, to provide a fast response. Fourth, for intracellular study, the sensor should be derivatizable into a cell-permeable form that can penetrate through the cell membrane and be hydrolyzed intracellularly to afford the sensor, which is then trapped in the cell. Fifth, their affinity for Zn^{2+} should be appropriate for the Zn^{2+} concentration range of interest.

We previously showed that ZnAFs, which satisfy most of the requirements mentioned above, can serve as useful tools for biological applications.[19,22] However, the affinity for Zn^{2+} remains an issue. To follow changes of Zn^{2+} concentration, it is desirable to use a sensor molecule whose apparent dissociation constant (K_d) is near the target concentration of Zn^{2+}. Almost all Zn^{2+} sensor molecules recently developed have K_d values in the nanomolar region (ZnAF-2, 2.7 nM), because cytosolic free Zn^{2+} concentration is controlled at ~1 nM or lower.[7] Neither Zn^{2+} deficiency nor Zn^{2+} excess affects cell viability and function,[23] and these sensors can easily be used in cytoplasm, etc. However, at higher concentrations of Zn^{2+}, the fluorescence intensity of these sensors would be saturated. Zn^{2+} is known to be sequestered in synaptic vesicles of many excitatory forebrain neurons, and the concentration of Zn^{2+} inside the vesicle was reported to be in the micro- to millimolar range.[8] This vesicular Zn^{2+} is also released into synaptic space, where it is estimated to achieve peak levels of 10−30 μM.[24] In such circumstances, sensor molecules with high affinity would have no ability to detect changes of Zn^{2+} concentration. So, for precise analysis of the biological roles of Zn^{2+}, we require a range of sensor molecules with K_d values not only in the nM range, but also higher.

Among Zn^{2+} sensor molecules so far reported, only Newport Green ($K_d \sim 1$ μM) has been used as a low-affinity Zn^{2+} sensor to detect synaptically released Zn^{2+}, for which purpose the Zn^{2+} concentration was calculated on the basis of the K_d value.[24] There is little other evidence to support the idea that the release of Zn^{2+} reaches micromolar levels, so confirmation remains desirable.

Our purpose in this study is to develop a range of low-affinity sensor molecules whose K_d values are higher than nanomolar order without any loss of favorable characteristics, such as low basal fluorescence and selectivity for Zn^{2+}.

In designing low-affinity sensor molecules, we chose ZnAF-2 as a basal structure. ZnAF-2 has a fluorescein fluorophore conjugated to *N*,*N*-bis(2-pyridylmethyl)ethylenediamine as a Zn^{2+} chelator. The design of the chelator was based on the structure of TPEN (*N*,*N*,*N*′,*N*′-tetrakis(2-pyridylmethyl)ethylenediamine). These groups offer the following advantages. Derivatives of fluorescein that are amino-substituted at the benzoic acid moiety emit little fluorescence due to the photo-induced electron transfer (PeT) quenching pathway, resulting in low basal fluorescence and high sensitivity.[20a] TPEN is known as a selective chelator of Zn^{2+} over Ca^{2+} or Mg^{2+}.[25] For intracellular application, a cell-permeant form can be obtained readily, because the TPEN moiety itself cannot be protonated at physiological pH, so the sensor remains intact. Moreover, the structural separation of sensor and chelator moieties means that modification of the chelator should not affect the fluorescence properties, such as maximum/minimum quantum yield or excitation/emission wavelength. This approach, leaving the fluorophore intact, is a characteristic advantage of fluorescent sensors utilizing the PeT mechanism. Therefore, we set out to develop a series of Zn^{2+} sensor molecules by modification of

(12) (a) Budde, T.; Minta, A.; White, J. A.; Kay, A. R. *Neuroscience* **1997**, *79*, 347−358. (b) Nasir, M. S.; Fahrni, C. J.; Suhy, D. A.; Kolodsick, K. J.; Singer, C. P.; O'Halloran, T. V. *J. Biol. Inorg. Chem.* **1999**, *4*, 775−783. (c) Fahrni, C. J.; O'Halloran, T. V. *J. Am. Chem. Soc.* **1999**, *121*, 11448−11458. (d) Kimber, M. C.; Mahadevan, I. B.; Lincoln, S. F.; Ward, A. D.; Betts, W. H. *Aust. J. Chem.* **2001**, *54*, 43−49. (e) Pearce, D. A.; Jotterand, N.; Carrico, I. S.; Imperiali, B. *J. Am. Chem. Soc.* **2001**, *123*, 5160−5161. (f) Hendrickson, K. M.; Geue, J. P.; Wyness, O.; Lincoln, S. F.; Ward, A. D. *J. Am. Chem. Soc.* **2003**, *125*, 3889−3895.

(13) (a) Walkup, G. K.; Imperiali, B. *J. Am. Chem. Soc.* **1996**, *118*, 3053−3054. (b) Walkup, G. K.; Imperiali, B. *J. Am. Chem. Soc.* **1997**, *119*, 3443−3450. (c) Walkup, G. K.; Imperiali, B. *J. Org. Chem.* **1998**, *63*, 6727−6731. (d) Thompson, R. B.; Maliwal, B. P.; Fierke, C. A. *Anal. Chem.* **1998**, *70*, 1749−1754. (e) Barondeau, D. P.; Kassmann, C. J.; Tainer, J. A.; Getzoff, E. D. *J. Am. Chem. Soc.* **2002**, *124*, 3522−3524. (f) Hong, S. H.; Maret, W. *Proc. Natl. Acad. Sci. U.S.A.* **2003**, *100*, 2255−2260. (g) Shults, M. D.; Pearce, D. A.; Imperiali, B. *J. Am. Chem. Soc.* **2003**, *125*, 10591−10597.

(14) (a) Maruyama, S.; Kikuchi, K.; Hirano, T.; Urano, Y.; Nagano, T. *J. Am. Chem. Soc.* **2002**, *124*, 10650−10651. (b) Henary, M. M.; Fahrni, C. J. *J. Phys. Chem. A* **2002**, *106*, 5210−5220. (c) Taki, M.; Wolford, J. L.; O'Halloran, T. V. *J. Am. Chem. Soc.* **2004**, *126*, 712−713. (d) Henary, M. M.; Wu, Y. G.; Fahrni, C. I. *Che.−Eur. J.* **2004**, *10*, 3015−3025.

(15) (a) Hanaoka, K.; Kikuchi, K.; Kojima, H.; Urano, Y.; Nagano, T. *Angew. Chem., Int. Ed.* **2003**, *42*, 2996−2999. (b) Hanaoka, K.; Kikuchi, K.; Kojima, H.; Urano, Y.; Nagano, T. *J. Am. Chem. Soc.* **2004**, *126*, 12470−12476. (c) Lim, N. C.; Yao, L.; Freake, H. C.; Bruckner, C. *Bioorg. Med. Chem. Lett.* **2003**, *13*, 2251−2254. (d) Koutaka, H.; Kosuge, J.; Fukasaku, N.; Hirano, T.; Kikuchi, K.; Urano, Y.; Kojima, H.; Nagano, T. *Chem. Pharm. Bull.* **2004**, *52*, 700−703.

(16) Haugland, R. P. *Handbook of Fluorescent Probes and Research Products*; 8th ed.; Molecular Probes, Inc.: Eugene, OR, 2001.

(17) (a) Walkup, G. K.; Burdette, S. C.; Lippard, S. J.; Tsien, R. Y. *J. Am. Chem. Soc.* **2000**, *122*, 5644−5645. (b) Burdette, S. C.; Walkup, G. K.; Spingler, B.; Tsien, R. Y.; Lippard, S. J. *J. Am. Chem. Soc.* **2001**, *123*, 7831−7841. (c) Burdette, S. C.; Frederickson, C. J.; Bu, W. M.; Lippard, S. J. *J. Am. Chem. Soc.* **2003**, *125*, 1778−1787. (d) Nolan, E. M.; Burdette, S. C.; Harvey, J. H.; Hilderbrand, S. A.; Lippard, S. J. *Inorg. Chem.* **2004**, *43*, 2624−2635. (e) Chang, C. J.; Nolan, E. M.; Jaworski, J.; Burdette, S. C.; Sheng, M.; Lippard, S. J. *Chem. Biol.* **2004**, *11*, 203−210. (f) Chang, C. J.; Nolan, E. M.; Jaworski, J.; Okamoto, K. I.; Hayashi, Y.; Sheng, M.; Lippard, S. J. *Inorg. Chem.* **2004**, *43*, 6774−6779.

(18) (a) Gee, K. R.; Zhou, Z. L.; Ton-That, D.; Sensi, S. L.; Weiss, J. H. *Cell Calcium* **2002**, *31*, 245−251. (b)Gee, K. R.; Zhou, Z. L.; Qian, W. J.; Kennedy, R. *J. Am. Chem. Soc.* **2002**, *124*, 776−778.

(19) (a) Hirano, T.; Kikuchi, K.; Urano, Y.; Higuchi, T.; Nagano, T. *J. Am. Chem. Soc.* **2000**, *122*, 12399−12400. (b) Hirano, T.; Kikuchi, K.; Urano, Y.; Nagano, T. *J. Am. Chem. Soc.* **2002**, *124*, 6555−6562.

(20) (a) Hirano, T.; Kikuchi, K.; Urano, Y.; Higuchi, T.; Nagano, T. *Angew. Chem.-Int. Edit.* **2000**, *39*, 1052−1054. (b) Sensi, S. L.; Ton-That, D.; Weiss, J. H.; Rothe, A.; Gee, K. R. *Cell Calcium* **2003**, *34*, 281−284. (c) Chang, C. J.; Jaworski, J.; Nolan, E. M.; Sheng, M.; Lippard, S. J. *Proc. Natl. Acad. Sci. U.S.A.* **2004**, *101*, 1129−1134.

(21) (a) Frederickson, C. *Sci. STKE* **2003**, *182*, 18. (b) Jiang, P. J.; Guo, Z. J. *Coord. Chem. Rev.* **2004**, *248*, 205−229. (c) Kikuchi, K.; Komatsu, K.; Nagano, T. *Curr. Opin. Chem. Biol.* **2004**, *8*, 182−191.

(22) Ueno, S.; Tsukamoto, M.; Hirano, T.; Kikuchi, K.; Yamada, M. K.; Nishiyama, N.; Nagano, T.; Matsuki, N.; Ikegaya, Y. *J. Cell Biol.* **2002**, *158*, 215−220.

(23) (a) MacDiarmid, C. W.; Milanick, M. A.; Eide, D. J. *J. Biol. Chem.* **2003**, *278*, 15065−15072. (b) Colvin, R. A.; Fontaine, C. P.; Laskowski, M.; Thomas, D. *Eur. J. Pharmacol.* **2003**, *479*, 171−185.

(24) (a) Li, Y.; Hough, C. J.; Suh, S. W.; Sarvey, J. M.; Frederickson, C. J. *J. Neurophysiol.* **2001**, *86*, 2597−2604. (b) Li, Y.; Hough, C. J.; Frederickson, C. J.; Sarvey, J. M. *J. Neurosci.* **2001**, *21*, 8015−8025.

(25) Arslan, P.; Divirgilio, F.; Beltrame, M.; Tsien, R. Y.; Pozzan, T. *J. Biol. Chem.* **1985**, *260*, 2719−2727.

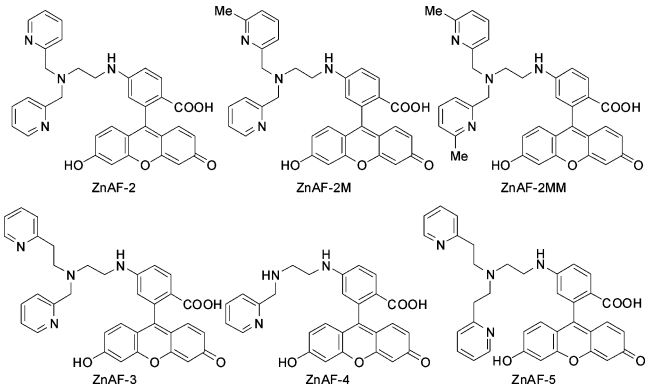

Figure 1. Structures of ZnAF family members. ZnAF-2 was previously reported to visualize Zn^{2+} in brain slices. The other sensor molecules were newly synthesized.

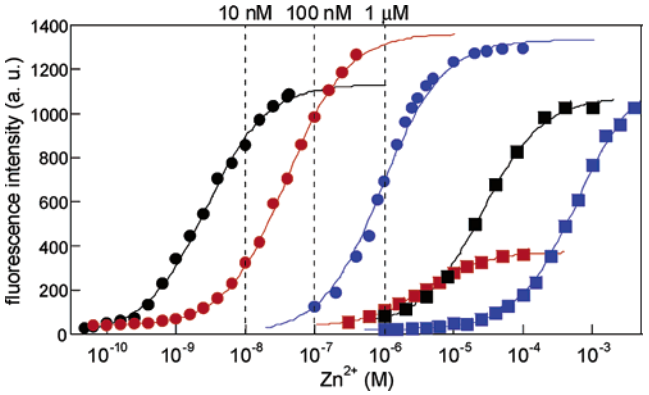

Figure 2. Changes of fluorescence intensity for 1 μM ZnAFs (ZnAF-2, black circle; ZnAF-2M, red circle; ZnAF-2MM, red square; ZnAF-3, blue circle; ZnAF-4, black square; and ZnAF-5, blue square) as a function of the concentration of free Zn^{2+} in 100 mM HEPES buffer (pH 7.4, $I = 0.1$ ($NaNO_3$)).

the TPEN moiety to obtain various K_d values without affecting the selectivity against other ions.

Here, we report a series of fluorescent sensor molecules for Zn^{2+} with various K_d values from nanomolar up to millimolar range. Their design, synthesis, and fluorescence properties are described. We also present applications to cultured cells and hippocampal slices.

Results and Discussion

Design and Synthesis. Figure 1 illustrates the structures of Zn^{2+} sensor molecules, ZnAF-2 and its new derivatives. ZnAF-2 was synthesized by conjugating 5-aminofluorescein and dipicolylamine via a linker, dibromoethane, so we introduced various chelators instead of dipicolylamine and left the fluorophore unchanged. The design was based on three strategies. First, we introduced steric hindrance at the nitrogen atom on the pyridine ring by substituting a methyl group at the 6-position (ZnAF-2M, ZnAF-2MM). Second, we removed one ligand, picolylamine (ZnAF-4). Last, we increased the distance between the ligands (ZnAF-3, ZnAF-5). The synthetic schemes for these sensors are described in the Supporting Information.

Fluorescence Properties. We measured the fluorescence intensity of these sensor molecules in various concentrations of Zn^{2+}. As we had expected, these sensors showed changes in fluorescence intensity at higher Zn^{2+} concentrations than ZnAF-2 (Figure 2) but retained almost the same fluorescence properties, such as absorption/emission wavelength and maximum/minimum quantum yield, which is convenient when using and comparing several sensors (Table 1). In each case, the fluorescence increase fitted well with a 1:1 binding model and the Hill coefficient of 1 suggests that a 1:1 Zn^{2+}−ZnAF complex was formed. The apparent dissociation constants were as follows: ZnAF-2M, 38 nM; ZnAF-2MM, 3.9 μM; ZnAF-3, 0.79 μM; ZnAF-4, 25 μM; and ZnAF-5, 0.60 mM (Table 2). Thus, we can follow a wide Zn^{2+} concentration range from 10^{-10} M up to 10^{-3} M by using different sensor molecules. Furthermore, by using them in combination, we can easily estimate the Zn^{2+} concentration. For example, if the concentration of free Zn^{2+} is 10 nM, there is strong fluorescence in ZnAF-2, weak fluorescence in ZnAF-2M, and no fluorescence in ZnAF-3 (Figure 2). At 100 nM Zn^{2+}, there is strong fluorescence in both ZnAF-2 and ZnAF-2M and little or no fluorescence in ZnAF-3. At 1 μM Zn^{2+}, there is strong fluorescence in ZnAF-3 and no fluorescence in ZnAF-4.

Among these sensors, ZnAF-2MM has lower quantum yield and fluorescence intensity in the presence of Zn^{2+} than the others. The fluorescence enhancement of ZnAFs, we consider, is attained through Zn^{2+} coordination to the amine on the benzoic acid moiety of fluorescein. In the absence of Zn^{2+}, the fluorescence is quenched due to the PeT from the benzoic acid moiety to the xanthene moiety. However, Zn^{2+} coordination alters the HOMO energy level of the benzoic acid moiety, thereby preventing PeT and leading to the enhancement of fluorescence from the xanthene moiety (fluorophore).[26] In ZnAF-2MM, the two methyl groups may alter the coordination structure of the Zn^{2+}−ZnAF complex, in a way that less strongly affects the HOMO energy level of the benzoic acid moiety, resulting in weak fluorescence.

Thus, we have completed developing a range of Zn^{2+} sensor molecules with various affinities for Zn^{2+} but whose fluorescence properties resemble those of ZnAF-2.

Determination of Complexing Rate. We then measured the complexing rate of these sensor molecules (Figure 3). When an excess amount of Zn^{2+} was added, all the sensors synthesized showed very rapid saturation of the fluorescence signal within about 100 ms, except for ZnAF-2MM, which reached maximum fluorescence after 1 s. Therefore, these sensors except for ZnAF-2MM are suitable for detecting rapid change in cellular Zn^{2+} concentration. The calculated association (k_{on}) and dissociation (k_{off}) constants are shown in Table 2. The k_{on} values of ZnAF-2M, ZnAF-3, and ZnAF-4 are almost the same as that of ZnAF-2, and the k_{off} values are larger than that of ZnAF-2, implying that these sensors can detect Zn^{2+} increase as fast as ZnAF-2 and Zn^{2+} decrease faster than ZnAF-2. ZnAF-2MM and ZnAF-5 have smaller k_{on} values than ZnAF-2. Apparently, just one picolyl group is important for the sensor to make a rapid complex with Zn^{2+}. On the other hand, the k_{off} values of ZnAFs are strongly dependent on the Zn^{2+} chelating structure. The k_{off} values of higher affinity sensors, such as ZnAF-2 or ZnAF-2M, may be relatively small but are not too slow for reversible assay of Zn^{2+} concentration. It is also clear that low-affinity sensors are more suitable for monitoring Zn^{2+} in a reversible fashion because of their large k_{off} values.

Metal Ion Selectivity. Figure 4 illustrates the fluorescence intensity of ZnAFs in the presence of various metal ions. Like

(26) Miura, T.; Urano, Y.; Tanaka, K.; Nagano, T.; Ohkubo, K.; Fukuzumi, S. *J. Am. Chem. Soc.* **2003**, *125*, 8666−8671.

Table 1. Absorbance and Fluorescence Properties of ZnAFs at pH 7.4[a]

	free			+Zn^{2+}		
Dye	λ_{max}	ϵ[b]	Φ[c]	λ_{max}	ϵ[b]	Φ[c]
ZnAF-2	490	7.8×10^4	0.023	492	7.6×10^4	0.3 2
ZnAF-2M	490	5.3×10^4	0.034	492	5.2×10^4	0.2 7
ZnAF-2MM	490	1.1×10^5	0.006	493	8.8×10^4	0.1 0
ZnAF-3	490	7.1×10^4	0.029	493	6.2×10^4	0.3 8
ZnAF-4	490	6.8×10^4	0.012	492	6.4×10^4	0.2 2
ZnAF-5	490	6.4×10^4	0.004	492	4.3×10^4	0.2 1

[a] All data were measured in 100 mM HEPES buffer (pH 7.4, $I = 0.1$ ($NaNO_3$)). [b] ϵ stands for extinction coefficient (M^{-1} cm^{-1}) measured at each λ_{max}. [c] Φ stands for quantum yield of fluorescence, determined using that of fluorescein (0.85) in 0.1 M NaOH aq. as a standard.

Table 2. Apparent Dissociation Constants (K_d) and Association and Dissociation Rate Constants (k_{on} and k_{off}) of ZnAFs in 100 mM HEPES Buffer (pH 7.4, $I = 0.1$ ($NaNO_3$)) at 25 °C

dye	K_d (M)	k_{on} (M^{-1} s^{-1})	k_{off} (s^{-1})
ZnAF-2	2.7×10^{-9}	3.1×10^6	8.4×10^{-3}
ZnAF-2M	3.8×10^{-8}	1.3×10^6	4.9×10^{-2}
ZnAF-2MM	3.9×10^{-6}	6.9×10^4	0.28
ZnAF-3	7.9×10^{-7}	1.4×10^6	1.1
ZnAF-4	2.5×10^{-5}	1.6×10^6	51
ZnAF-5	6.0×10^{-4}	6.7×10^4	40

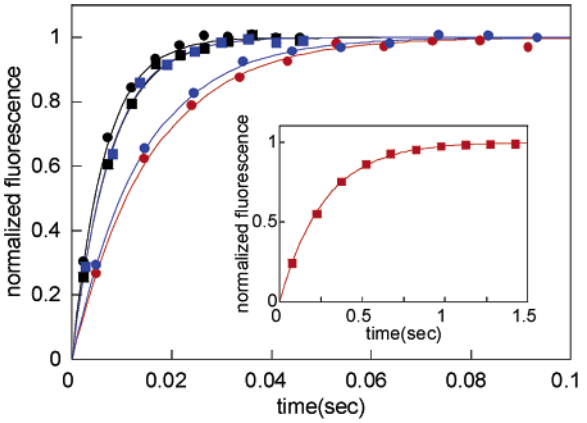

Figure 3. Time course measurement of the fluorescence intensity for 1 μM ZnAFs after mixing with Zn^{2+}. 50 μM Zn^{2+} was mixed with ZnAF-2 (black circle), ZnAF-2M (red circle), ZnAF-2MM (red square), and ZnAF-3 (blue circle). 1 mM Zn^{2+} was mixed with ZnAF-4 (black square) and ZnAF-5 (blue square). These data were measured in 100 mM HEPES buffer (pH 7.4, $I = 0.1$ ($NaNO_3$)) and 25 °C.

ZnAF-2, they show no response to biologically important metal ions, such as Ca^{2+} and Mg^{2+}, at millimolar concentration. Thus, the sensors with lower affinity for Zn^{2+} do not show reduced selectivity for Zn^{2+}. All the sensors have the same coordination atoms, and we think that this metal ion selectivity is mainly due to the character of nitrogen atom on the pyridine ring. In hard and soft acids and bases (HSAB) theory, pyridine is classified as a borderline base. It prefers Zn^{2+} to Ca^{2+} or Mg^{2+}, which is a hard acid. This preference would be important for the determination of the metal ion selectivity of ZnAFs. Some sensors show an increase in fluorescence intensity in the presence of some transition metals other than Zn^{2+}. Above all, Cd^{2+} shows a similar response to Zn^{2+}. However Cd^{2+} is rarely present in biological systems, so there would be no difficulty in biological applications.

Effect of pH. In addition to metal ion selectivity, it is important for many biological applications that the sensor does not respond to changes in pH. We measured the fluorescence intensity of ZnAFs at various pH values (Supporting Information, Figure S7). As in the case of ZnAF-2, the free bases of these sensors exhibit no significant emission enhancement upon acidification. Thus, the basal fluorescence intensity should be little affected by physiological pH changes.

Measuring Intracellular Zn^{2+}. We applied these sensor molecules to cultured cells or hippocampal slices. First, we measured the intracellular Zn^{2+} concentration of CHO cells to show their utility in fluorescence microscopic imaging by using membrane-permeable acetyl ester derivatives of ZnAF, ZnAF-2 DA,[19] and ZnAF-3 DA. These nonpolar compounds can easily penetrate through the cell membrane into the cytosol, where the acetyl groups are hydrolyzed by esterase to afford the Zn^{2+} sensors. After incubation with 10 μM sensors, cells showed weak fluorescence, suggesting that these sensors can be used intracellularly (data not shown). Then, we examined whether the difference of affinity is reflected in the fluorescence microscopic imaging of intracellular Zn^{2+} or not. The intracellular concentration of Zn^{2+} was controlled with a Zn^{2+} ionophore, pyrithione (2-mercaptopyridine *N*-oxide), which brings extracellular Zn^{2+} into the cytoplasm. We added various concentrations of Zn^{2+} with pyrithione, and the intracellular Zn^{2+} concentration was measured by fluorescence microscopy. Figure 5 shows the fluorescence response of each sensor molecule. With the increase of extracellular Zn^{2+} concentration from 0.3 to 300 μM, the fluorescence intensity of ZnAF-2 ($K_d = 2.7$ nM) was soon saturated. On the other hand, that of ZnAF-3 ($K_d = 0.79$ μM) was not saturated until 300 μM Zn^{2+}. This different response was clearly derived from the different affinity of the two sensors for Zn^{2+}. ZnAF-2 is superior for detecting lower Zn^{2+} concentrations, while ZnAF-3 can measure higher Zn^{2+} concentrations, which shows the importance of affinity for Zn^{2+} in cellular imaging. Thus, we can trace intracellular Zn^{2+} accurately by using combinations of several sensor molecules.

These results are in contrast with a previous report,[27] in which affinity for Zn^{2+} was suggested to be of less importance than dye concentration in fluorescence imaging; i.e., the dye concentration dominates the sensitivity of the reporting system. If the dye concentration is relatively high compared with the total ion pool available, the calibration of the dye signal to ion concentration may be affected, so care is necessary when using high intracellular dye concentrations. However, we consider that affinity is always an important factor in fluorescence imaging, as we have shown here. Using Zn^{2+} sensor molecules with suitable affinities should allow better calibration of the fluorescent signal to Zn^{2+} concentration.

(27) Dineley, K. E.; Malaiyandi, L. M.; Reynolds, I. J. *Mol. Pharmacol.* **2002**, *62*, 618−627.

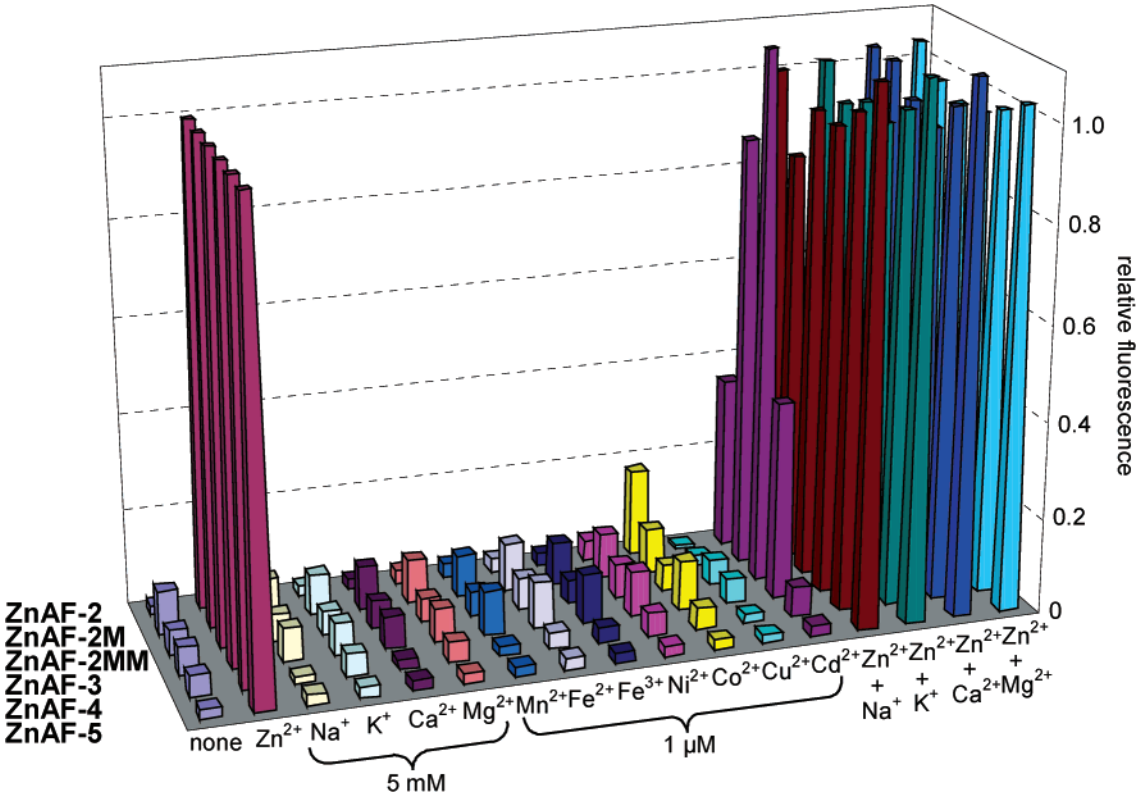

Figure 4. Relative fluorescence intensity of 1 μM ZnAFs in the presence of various metal ions. Na^+, K^+, Ca^{2+}, and Mg^{2+} were added at the concentration of 5 mM. Zn^{2+} was added at either 1 μM (ZnAF-2, ZnAF-2M) or 10 μM (ZnAF-2MM, ZnAF-3) or 100 μM (ZnAF-4, ZnAF-5). Other metals were added at 1 μM. These data were measured in 100 mM HEPES buffer (pH 7.4, $I = 0.1$ ($NaNO_3$)).

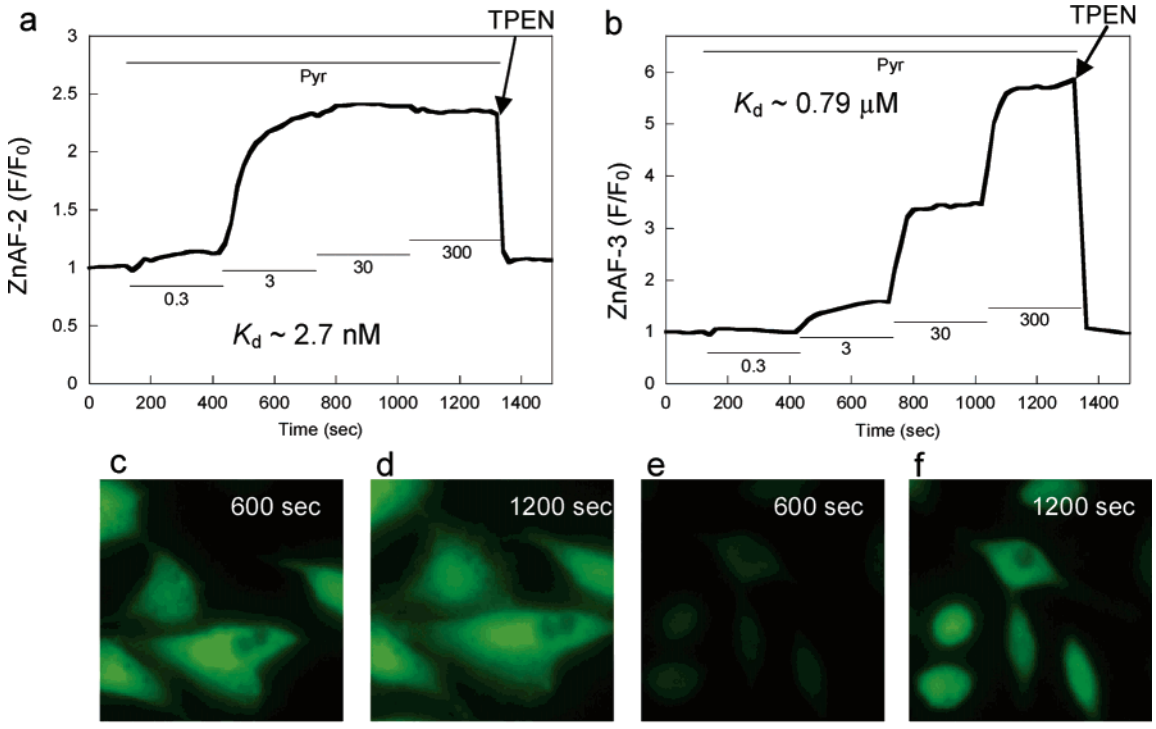

Figure 5. Fluorescence response of ZnAFs induced by intracellular Zn^{2+}. CHO cells incubated with 10 μM ZnAF-2 DA (a) or ZnAF-3 DA (b) for 30 min at room temperature were washed with PBS and fluorescence excited at 470−490 nm was measured at 20 s intervals. At 2 min, cells were exposed to pyrithione (Pyr, 100 μM) in the presence of sequentially increased concentrations of added extracellular Zn^{2+} (0.3, 3, 30, and 300 μM, each for 5 min) as indicated by the solid lines. Return of intracellular Zn^{2+} to the resting level was achieved by addition of TPEN (50 μM; starting at arrow). Fluorescence images incubated with ZnAF-2 DA (c, 600 s), (d, 1200 s), or ZnAF-3 DA (e, 600 s; f, 1200 s) are shown in the bottom panels.

Measuring Synaptically Released Zn^{2+}. For the analysis of Zn^{2+} in the central nervous system, we applied these sensors to hippocampal slices and measured synaptically released Zn^{2+} induced by membrane potential-depolarizing stimulation. All

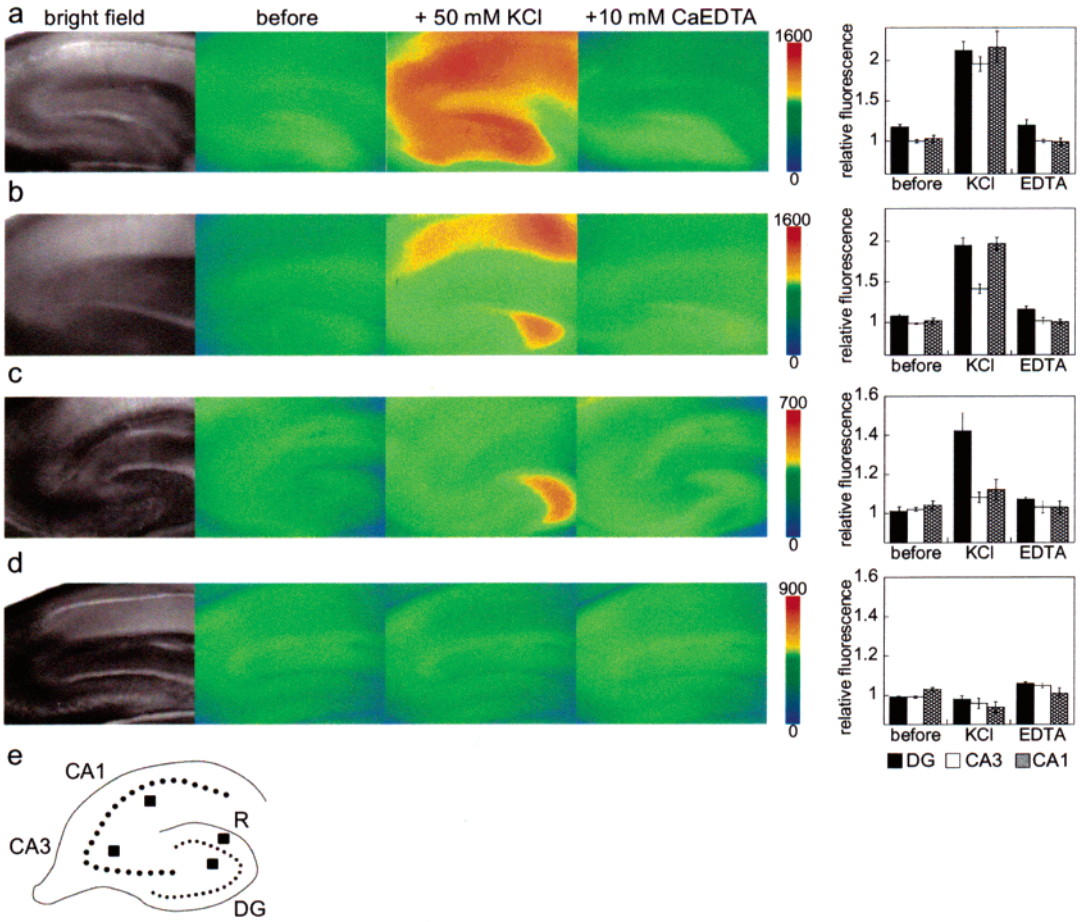

Figure 6. Fluorescence response of ZnAFs detecting extracellularly released Zn^{2+} in hippocampal slices. Fluorescence excited at 470−490 nm was measured soon after rat hippocampal slices were loaded with 1 μM ZnAF-2 (a), ZnAF-2M (b), ZnAF-3 (c), or ZnAF-4 (d). Then, 50 mM KCl (at 1 min) and 10 mM CaEDTA (at 10 min) were added to the imaging solution. Bright field images, fluorescence images at 0 min (before), at 3 min (+50 mM KCl), and at 15 min (+10 mM CaEDTA) are shown in each row. Relative fluorescence intensities of DG, CA3, and CA1 are shown in the bar graph, expressed as mean ± SE ($n = 3$ for ZnAF-2, ZnAF-3, and ZnAF-4 and $n = 5$ for ZnAF-2M). The bottom schematic (e) shows the approximate positions used for measurements of fluorescence intensity in the dentate gyrus (DG), CA3, CA1, and R (as a reference) region.

of the nerve terminals were stimulated into depolarization after addition of potassium ions. We observed a large fluorescence increase upon addition of 50 mM KCl to slices loaded with 1 μM ZnAF. To confirm that this fluorescence increase was due to an increase of extracellular Zn^{2+} concentration, we further added CaEDTA, an extracellular Zn^{2+} chelator. This treatment reduced the fluorescence intensity of ZnAF to the initial level, which confirmed that the indicator was responding to extracellular Zn^{2+} and that the extracellular Zn^{2+} concentration was below the detection level prior to depolarization. We acquired different fluorescence images after stimulation depending on the K_d value of the ZnAFs (Figure 6a−d). In the fluorescence imaging using ZnAF-2 ($K_d = 2.7$ nM), the fluorescence intensity increased mainly in three regions, the dentate gyrus (DG), CA3, and CA1, which were indistinguishable. Therefore, no regional difference of released Zn^{2+} concentration was observed using ZnAF-2, probably because of its high affinity for Zn^{2+}. With ZnAF-2M ($K_d = 38$ nM), on the other hand, the fluorescence intensity increased in DG and CA1, but increased less in CA3, and with ZnAF-3 ($K_d = 0.79$ μM), a fluorescence increase was seen only in DG. The lower affinity sensor, ZnAF-4 ($K_d = 25$ μM) showed no fluorescence increase. The mean increase of fluorescence intensity in each region is shown in the bar graph. So, these results demonstrate for the first time that a higher concentration of Zn^{2+} is released in DG than in CA3 or CA1, and a lower concentration of Zn^{2+} is released in CA3 than in DG or CA1.

A key advantage of using plural sensors is that estimation of the released Zn^{2+} concentration level is possible. In DG, there is a fluorescence response of ZnAF-3 ($K_d = 0.79$ μM) and no response of ZnAF-4 ($K_d = 25$ μM). Namely, the released Zn^{2+} concentration in DG is below the detection level for ZnAF-4. Thus, the released Zn^{2+} concentration is estimated to be of the order of 1 μM DG (Figure 2). Similarly, in both CA1 and CA3, there is a fluorescence response of ZnAF-2M ($K_d = 38$ nM) and no response of ZnAF-3. Thus, the released Zn^{2+} concentration level in CA1 and CA3 can be estimated to be of the order of 100 nM or less.

Thus, by using dyes with different affinity for Zn^{2+} for fluorescence imaging, we can obtain considerably more information from the same sample than would be possible with a single dye. Furthermore, it is clear that there is no single K_d value suitable for tracing all of the concentration levels of synaptically released Zn^{2+}, because a K_d value suitable for one region would give either no response or a saturated fluorescence signal in other regions. So, the importance of using several sensor molecules is clear, just as we had anticipated when designing this range of sensors. By virtue of having a spectrum

of affinities for Zn^{2+}, ZnAFs are the first Zn^{2+} sensor molecules not only to reveal regional differences but also to allow estimation of the concentrations of synaptically released Zn^{2+} in hippocampal slices. In addition, ZnAFs are also suitable for analyzing temporal changes of Zn^{2+}; a fast fluorescence increase and decrease in the CA1 region was visualized with ZnAF-2M (data not shown).

Previous reports indicate that electrical stimulation and potassium stimulation produce similar responses in terms of released Zn^{2+} concentration.[24] This would suggest that a similar concentration level of Zn^{2+} is released during natural neuronal activity. However, the reported concentration levels of released Zn^{2+} vary drastically. Li et al. suggested that synaptic release of Zn^{2+} during stimulation reaches micromolar levels.[24] They used the fluorescent sensor molecule Newport Green, which has an affinity of $\sim$1 μM for Zn^{2+}. On the other hand, Kay examined synaptic release of Zn^{2+} using another fluorescent sensor molecule, FluoZin-3, whose K_d value is 15 nM and concluded that little Zn^{2+} ($\sim$6 nM) was released during stimulation.[28] Both estimations were done with a single sensor molecule, with quite different K_d values, and they utilized the maximum and minimum fluorescence intensity for Zn^{2+} calibration. However, our estimation is based on the use of several sensor molecules without relying on measurements of maximum or minimum fluorescence intensity. Moreover, our sensors have similar fluorescence properties, and only their affinity for Zn^{2+} differs. We think these features support the reliability of Zn^{2+} estimation with ZnAFs.

On the basis of the above results, our ZnAFs introduced here are expected to become useful tools in the investigation of Zn^{2+} biology, especially the role of Zn^{2+} in the central nervous system.[2d] These ZnAFs should have a wide range of application. In addition to synaptic release of Zn^{2+}, Zn^{2+} is suggested to be involved in excitotoxic neuronal death after head trauma, epilepsy, and cerebral ischemia and reperfusion.[29] Recently, extracellular accumulation of Zn^{2+} during ischemia and reperfusion was reported.[30] However, regional differences of Zn^{2+} over the areas of DG, CA3, and CA1 were not observed. Zn^{2+} sensor molecules with suitable K_d values may visualize regional differences, allowing detailed analysis of the Zn^{2+} distribution.

Although other Zn^{2+} sensor molecules with various affinities are available,[11g,13d] ZnAFs are the first sensor molecules suitable for both intra- and extracellular applications in biology. Combined with fluorescence microscopic imaging, ZnAFs have the potential to play a central role in the investigation of Zn^{2+} biology.

Conclusion

We have developed a range of fluorescent Zn^{2+} sensor molecules, ZnAF-2M, ZnAF-2MM, ZnAF-3, ZnAF-4, and ZnAF-5, whose K_d values range from nanomolar to subnanomolar levels. They all have similar fluorescence properties and differ only in their affinity for Zn^{2+}, without any loss of selectivity for Zn^{2+}. Using ZnAF-2 DA and ZnAF-3 DA, cell-permeable derivatives of ZnAFs, different responses to changes in intracellular Zn^{2+} concentration were observed. Extracellular Zn^{2+} release was also measured using ZnAFs and their use enabled us to detect regional difference in the Zn^{2+} release for the first time, as well as to estimate the approximate concentration of synaptically released Zn^{2+} in hippocampal slices. We can measure Zn^{2+} concentration over a wide range by using ZnAFs, which are expected to be useful probes for obtaining further insight into the physiological importance of Zn^{2+}.

Experimental Section

General Information. All reagents and solvents were of the highest commercial quality and were used without purification. ZnAF-2 and ZnAF-2 DA were purchased from Daiichi Pure Chemicals Co., Ltd. (Tokyo, Japan). ZnAF-2M, ZnAF-2MM, ZnAF-3, ZnAF-4, ZnAF-5, and ZnAF-3 DA were prepared as described in the Supporting Information. Dimethyl sulfoxide (DMSO), 2-[4-(2-hydroxyethyl)-1-piperazinyl]ethanesulfonic acid (HEPES), nitrilotriacetic acid (NTA), and *N*,*N*,*N*′,*N*′-tetrakis-(2-pyridylmethyl)ethylenediamine (TPEN) were purchased from Dojindo Laboratories, Ltd. (Kumamoto, Japan). All other reagents were purchased from either Tokyo Kasei Kogyo Co., Ltd. (Tokyo, Japan), or Wako Pure Chemical Industries, Ltd. (Osaka, Japan).

Fluorometric Analysis. Fluorescence spectroscopic studies were performed with a Hitachi F4500 (Tokyo, Japan). The slit width was 2.5 nm for both excitation and emission. The photomultiplier voltage was 750 V. ZnAFs were dissolved in DMSO to obtain 10 mM stock solutions. Fluorescence intensities of 1 μM ZnAFs as a function of free Zn^{2+} concentration were measured in 100 mM HEPES buffer (pH 7.4, $I = 0.1$ ($NaNO_3$)). Free Zn^{2+} concentration was controlled by using 0−9 mM $ZnSO_4$/10 mM NTA (nitrilotriacetic acid) systems[19a] for ZnAF-2 and ZnAF-2M and unbuffered Zn^{2+} for other ZnAFs. The fluorescence intensity data were fitted to eq 1, and K_d was calculated, where F is the fluorescence intensity, F_{max} is the maximum fluorescence intensity, F_0 is the fluorescence intensity with no addition of Zn^{2+}, and $[Zn^{2+}]_f$ is the free Zn^{2+} concentration.

$$F = F_0 + (F_{max} - F_0)([Zn^{2+}]_f)/(K_d + [Zn^{2+}]_f) \quad (1)$$

Relative quantum yields of fluorescence were obtained by comparing the area under the corrected emission spectrum of the sample at 492 nm with that of a solution of fluorescein in 0.1 M NaOH (quantum yield: 0.85). UV−visible spectra were measured with a Shimadzu UV-1600 (Tokyo, Japan).

Stopped-Flow Measurements. Stopped-flow experiments were performed with a SF-61 DX2 double-mixing stopped-flow spectrofluorimeter (Hi-Tech, Salisbury, U.K.) equipped with a monochromator between the 75 W xenon light source and the reaction cuvette excitation window. The quartz sample cuvette and syringes containing the reactants were maintained at 25 ± 0.1 °C by a circulating water bath. The pneumatic cylinder was driven by a nitrogen pressure of 6 bar, which resulted in an instrument dead time of 1 ms. A solution of 2 μM ZnAF in 100 mM HEPES buffer (pH 7.4, $I = 0.1$ ($NaNO_3$)) was combined with an equal volume of 100 μM or 2 mM of $ZnSO_4$. Fluorescence was measured with excitation at 492 nm and with emission at >530 nm, using a 530 cutoff filter. The fluorescence intensity data were fitted to eq 2, and k_{obs} was obtained, where F is the normalized fluorescence. Then, k_{on} and k_{off} were calculated as described previously.[19b]

$$F = 1 - \exp(-k_{obs}t) \quad (2)$$

Imaging System. The imaging system was comprised of an inverted fluorescence microscope (IX-71; Olympus, Tokyo, Japan), CoolSNAP HQ CCD camera (Roper Scientific, Tucson, AZ), and an image processor (MetaFluor; Universal Imaging Corp., Downingtown, PA). The microscope was equipped with a xenon lamp (AH2-RX; Olympus), an objective lens for CHO cells (PlanApo 60×/1.40 oil; Olympus) or

(28) Kay, A. R. *J. Neurosci.* **2003**, *23*, 6847−6855.
(29) (a) Choi, D. W.; Koh, J. Y. *Annu. Rev. Neurosci.* **1998**, *21*, 347−375. (b) Frederickson, C. J.; Hernandez, M. D.; McGinty, J. F. *Brain Res.* **1989**, *480*, 317−321. (c) Suh, S. W.; Chen, J. W.; Motamedi, M.; Bell, B.; Listiak, K.; Pons, N. F.; Danscher, G.; Frederickson, C. J. *Brain Res.* **2000**, *852*, 268−273.
(30) Wei, G.; Hough, C. J.; Li, Y.; Sarvey, J. M. *Neuroscience* **2004**, *125*, 867−877.

for hippocampal slices (UPlanAPo 4×/0.16; Olympus), an excitation filter (BP470-490; Olympus), a dichroic mirror (DM505; Olympus), and an emission filter (BA510-550; Olympus).

Preparation of Cells. CHO cells were cultured in Alpha medium (αMEM; Invitrogen Corp., Carlsbad, CA) containing 10% fetal bovine serum (Invitrogen Corp.), 1% penicillin (Invitrogen), and 1% streptomycin (Invitrogen) at 37 °C in a 5/95 CO_2/air incubator. Cells were passaged 3 days before dye loading on a 35 mm glass-based dish (Iwaki, Funabashi, Japan). Then the cells were rinsed with phosphate-buffered saline (PBS; Invitrogen), and incubated with PBS containing 10 μM ZnAF-2 DA or ZnAF-3 DA for 30 min at 37 °C. The cells were washed with PBS twice and mounted on the microscope stage. Fluorescence excited at 470−490 nm was measured at 20 s intervals, and the responses of three cells were compiled to generate a single trace.

Preparation of Rat Hippocampal Slices. The whole brains of adult Wistar rats (male, 200−250 g) were removed quickly under ether anesthesia and placed in ice-cold ACSF (artificial cerebrospinal fluid), which was aerated with 95/5 O_2/CO_2. The composition of ACSF was 124 mM NaCl, 2.5 mM KCl, 26 mM $NaHCO_3$, 1.25 mM NaH_2PO_4, 2.0 mM $CaCl_2$, 1.0 mM $MgCl_2$, and 10 mM glucose. The hippocampus was isolated, placed on an agar plate, and sliced into 300 μm thick slices with a rotary slicer (Model DTY 7700; Dosaka Co., Osaka, Japan). The fresh hippocampal slices were incubated in ACSF equilibrated with 95/5 O_2/CO_2 for more than 30 min at room temperature. Then each slice was transferred to a chamber on the microscope, where it was held in place by a metal wire ring with a stretched nylon net.

Acknowledgment. This work was supported in part by the Ministry of Education, Culture, Sports, Science and Technology of Japan (Grants for The Advanced and Innovational Research Program in Life Sciences to T.N., 15681012 and 16048206 to K.Kikuchi). K.Kikuchi was also supported by the Sankyo Foundation, by the Kanagawa Academy of Science, and by the Suzuken Memorial Foundation.

Supporting Information Available: Synthetic details and characterization of ZnAF-2M, ZnAF-2MM, ZnAF-3, ZnAF-4, ZnAF-5, and ZnAF-3 DA (PDF). This material is available free of charge via the Internet at http://pubs.acs.org.

JA050301E